Data Repository item 2003167:

Orthogonal jointing during coeval igneous degassing and normal faulting, Yucca Mountain, Nevada

W. M. Dunne, D. A. Ferrill, J. G. Crider, B. E. Hill, D. J. Waiting, P. C. La Femina, A. P. Morris, R. W. Fedors

Geological Society of America Bulletin (2003)

Data Repository supplement prepared by J. G. Crider.

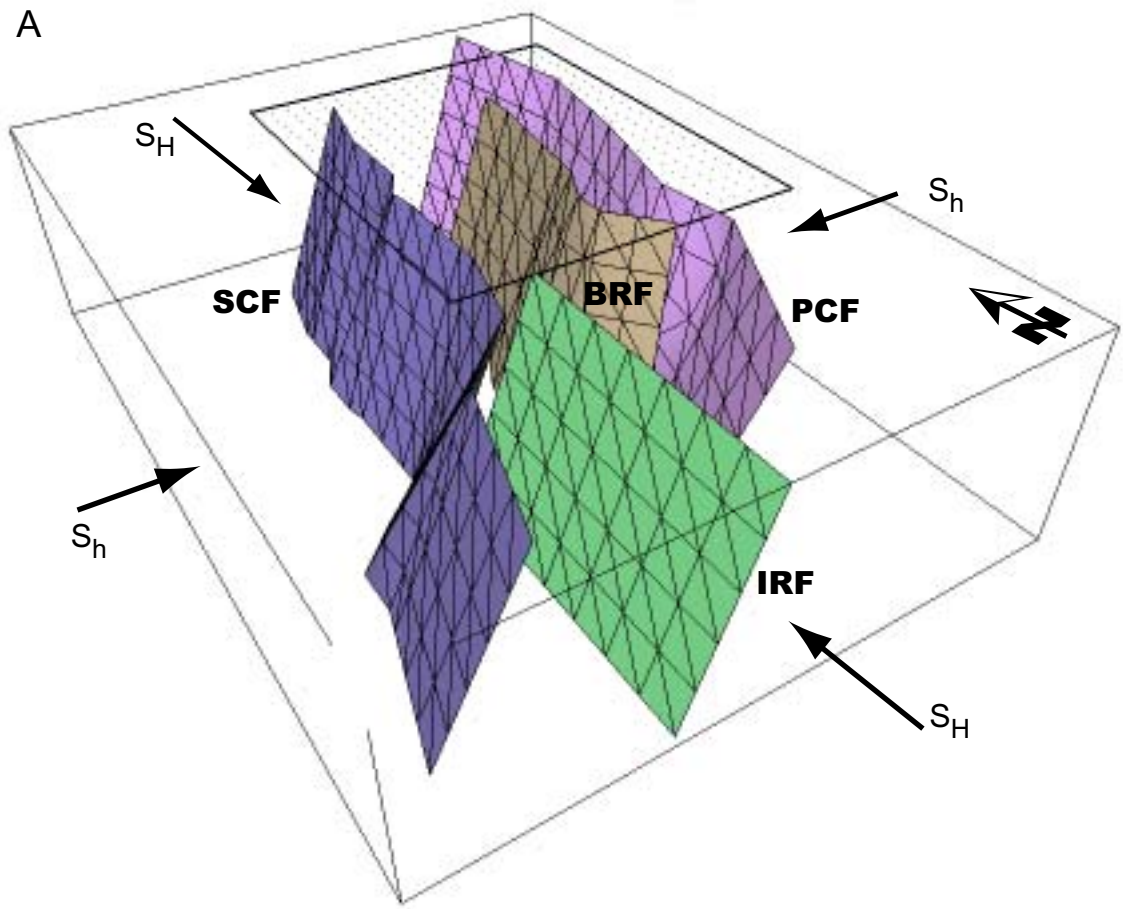

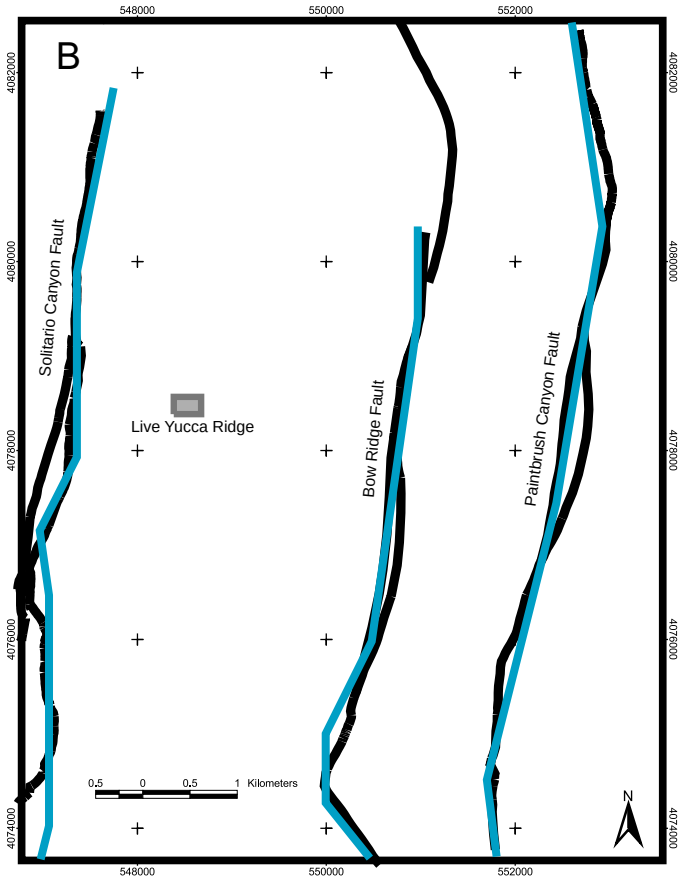

Figure DR1. Model configuration.
A. Perspective view of model fault geometry. SCF = Solitario Canyon Fault (blue), IRF = Iron Ridge Fault (green), BRF = Bow Ridge Fault (brown), PCF = Paintbrush Canyon Fault (purple). Arrows indicate the direction of maximum (S_H) and minimum (S_h) remote horizontal stresses. Surface traces of the faults are coincident with the free surface of the model elastic half space. Half-space is semi-infinite; bounding box is shown to illustrate perspective only. Dimensions of the bounding box are 14 km by 19 km by 5 km (east, north, depth). Rectangle at surface shows approximate area of B and Figs. DR5-DR7. Dots show calculation grid for principal stresses. **B.** Surface traces of modeled faults (light blue) compared to surface traces of mapped faults (black). Mapped fault traces after Day et al. (1998).

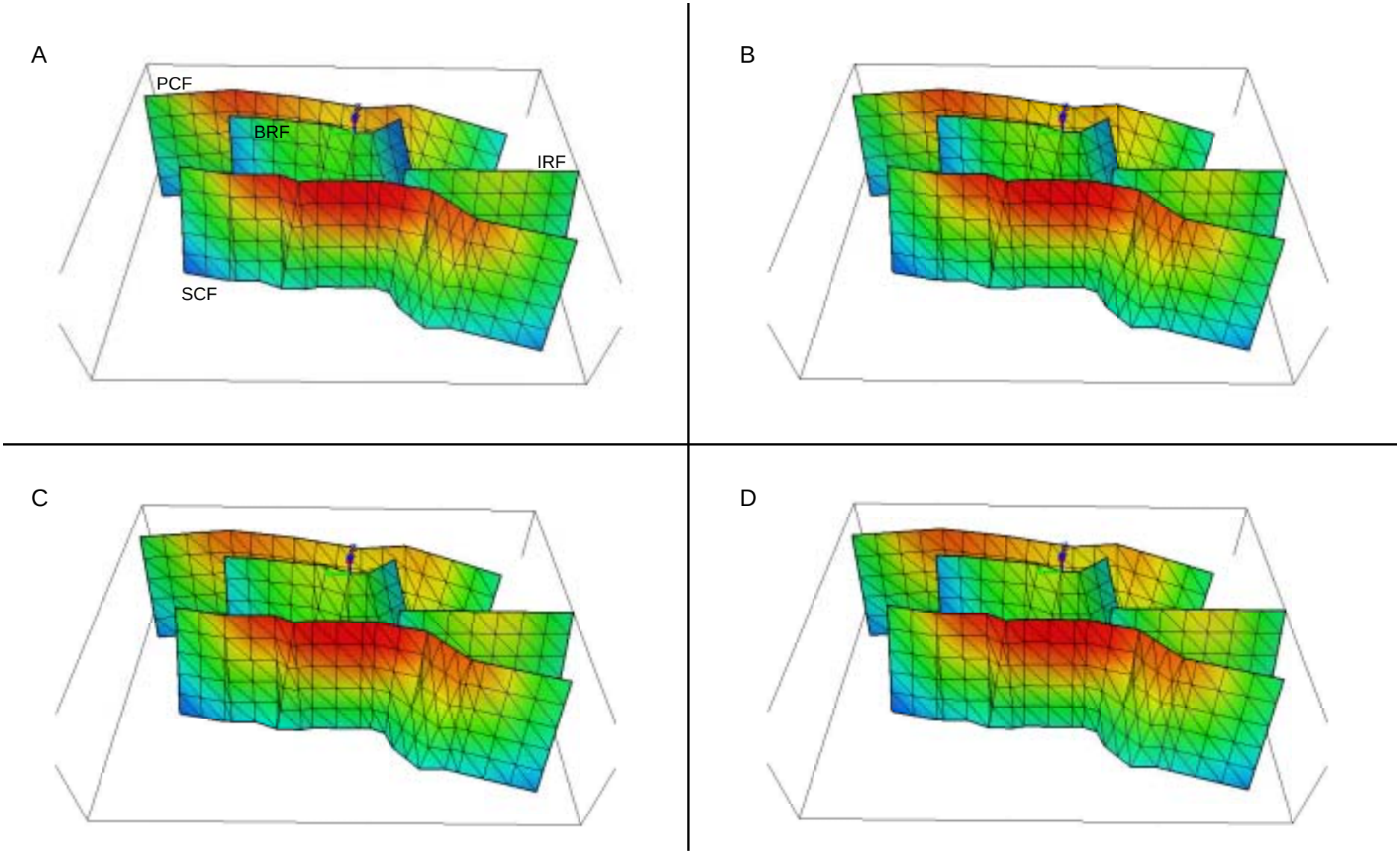

Figure DR2. East-facing perspective view of modeled faults with contours of modeled dip slip for four different stress boundary conditions. PCF = Paintbrush Canyon Fault, BRF = Bow Ridge Fault, IRF = Iron Ridge Fault, SCF = Solitario Canyon Fault. The color scale is the same for all four images: red = maximum dip slip (>1 m for these scenarios); blue = minimum dip slip (<0.1 m). The pattern of slip distribution is virtually the same for all four trials. In all cases the minium horizontal remote stress (S_h) is E-W and the maximum horizontal remote stress (S_H) is N-S. The vertical stress (S_V) is equivalent to the lithostatic load (L). The shear modulus for these trials is 30 GPa. **A.** S_h = L-10 MPa; $S_H = S_V$ = L **B.** S_h = L-10 MPa; S_H = L-4 MPa **C.** S_h = L-10 MPa; S_H = L-8 MPa (This is the scenario for which results are presented in the manuscript.) **D.** $S_h = S_H$ = L-10 MPa.

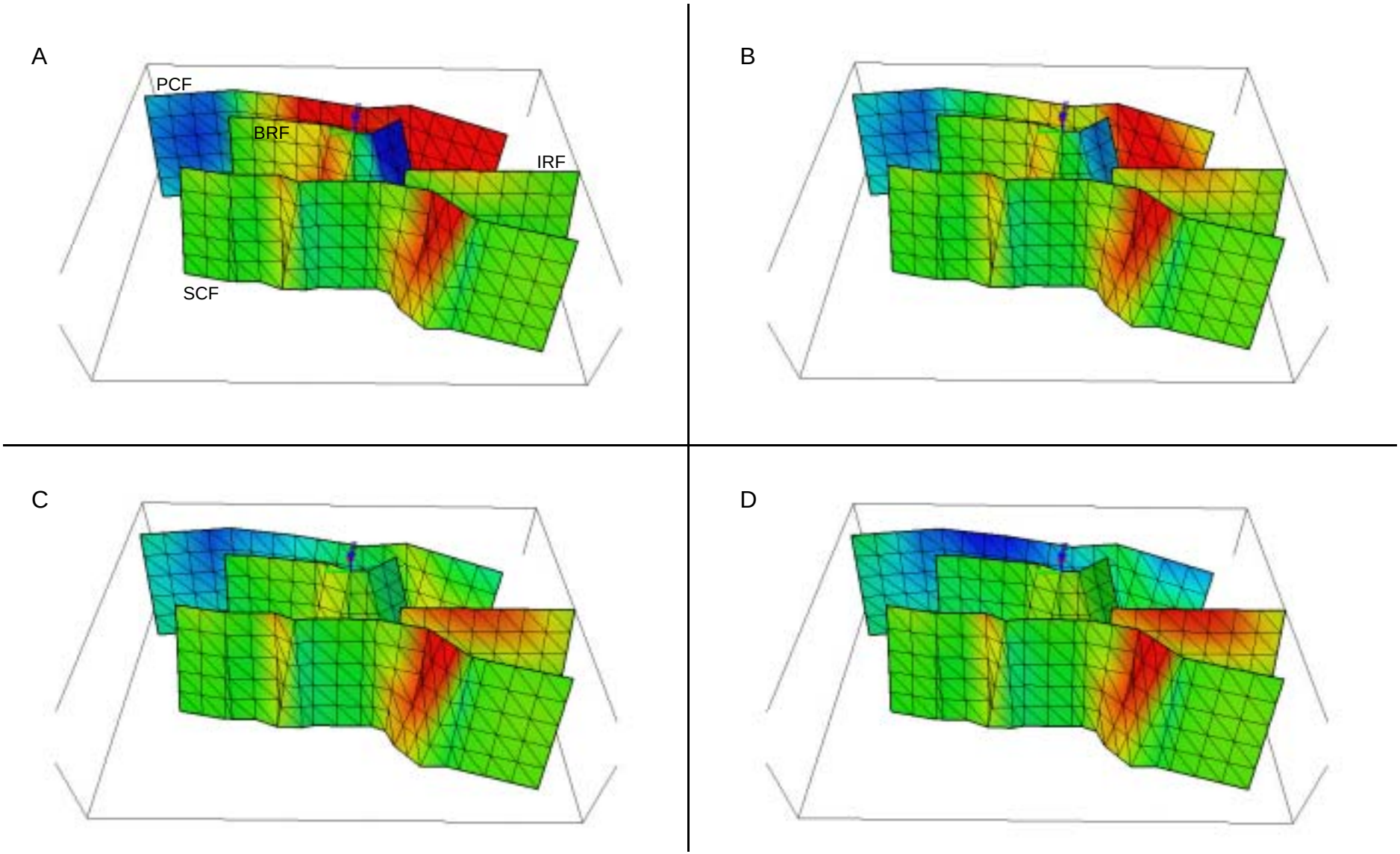

Figure DR3. East-facing perspective view of modeled faults with contours of modeled strike-parallel component of slip for the four trials shown in Fig. DR2. Labels as in Fig. DR2. The color scale is the same for all four images: red = maximum left-lateral slip (>0.2 m for these scenarios); blue = max. right-lateral slip (>0.2 m); green = no strike slip. Oblique slip is greater where the strike of the fault segment deviates from North. Note that these values are about an order of magnitude smaller than dip slip values. In all cases the minium horizontal remote stress (S_h) is E-W and the maximum horizontal remote stress (S_H) is N-S. The vertical stress (S_V) is equivalent to the lithostatic load (L). The shear modulus for these trials is 30 GPa. **A.** S_h = L-10 MPa; S_H = S_V = L **B.** S_h = L-10 MPa; S_H = L-4 MPa **C.** S_h = L=10 MPa; S_H = L-8 MPa (This is the scenario for which results are presented in the manuscript.) **D.** S_h = S_H = L-10 MPa.

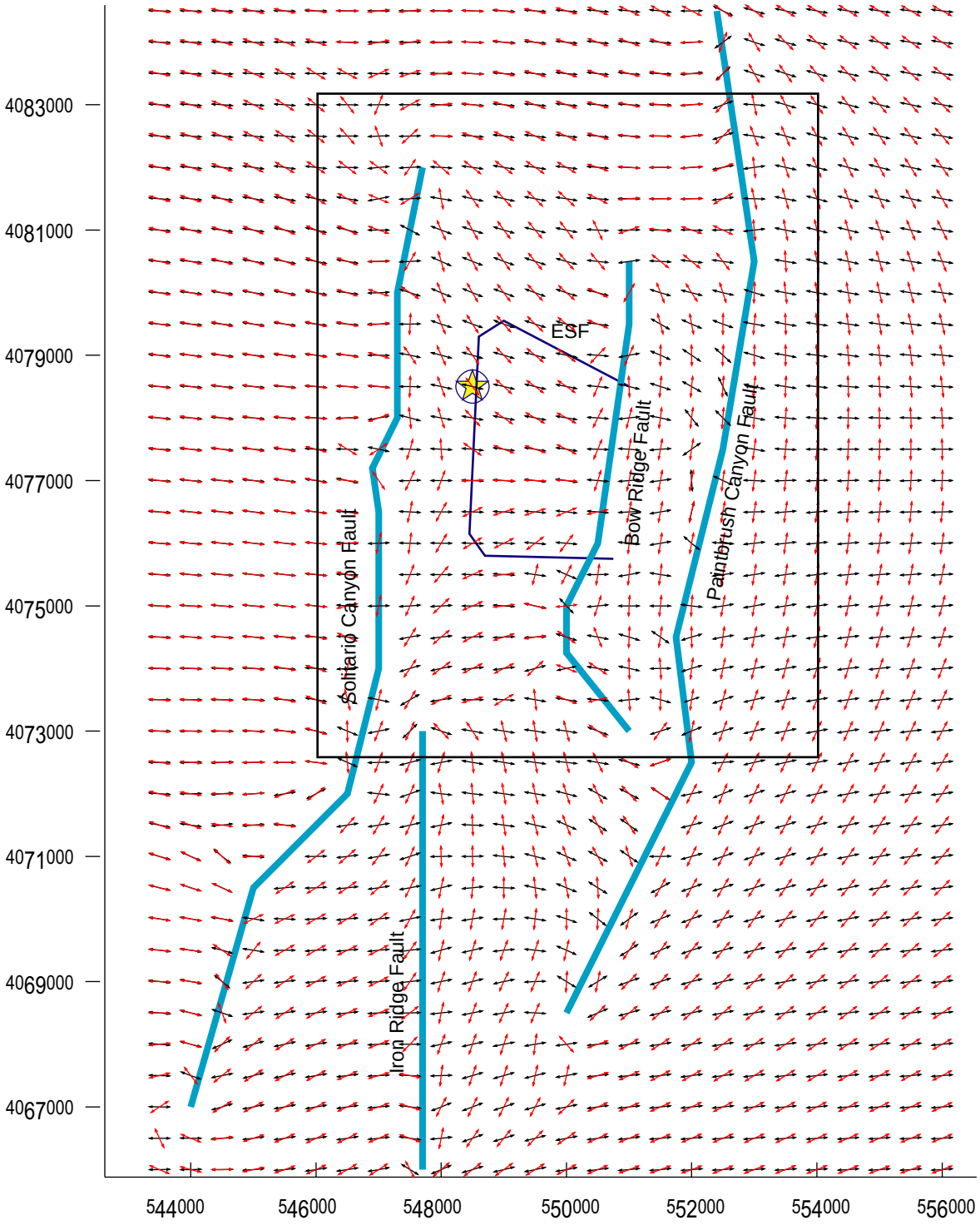

Figure DR4. Modeled direction of horizontal least principal stress (S_h) at 100 m depth for two different remote stress boundary conditions. In both cases the remote stresses are oriented such that S_h is E-W and S_H is N-S. The shear modulus is 30 GPa. Black arrows show results for remote S_h = L-10, and remote $S_H = S_V$ = L (case A in Figs. DR2 and DR3). Red arrows show results for remote S_h = L -10 and remote S_H = L-8 (case C in Figs. DR2 and DR3. These are the results presented in the manuscript). We expect joints to form perpendicular to the local least principal stress. Note that outside the faulted region, the expected joint orientations are primarily N-S (for example, in the hanging wall of the Solitario Canyon Fault) or E-W (for example, in the footwall of the Paintbrush Canyon Fault). In the blocks between faults or near the ends of the faults, the stress field has been perturbed so that expected joint orientations are oblique to the regional direction. ESF = Exploratory Studies Facility. Star shows location of Live Yucca Ridge. Box shows area of Figs DR5-DR7. Coordinates are in UTM (km).

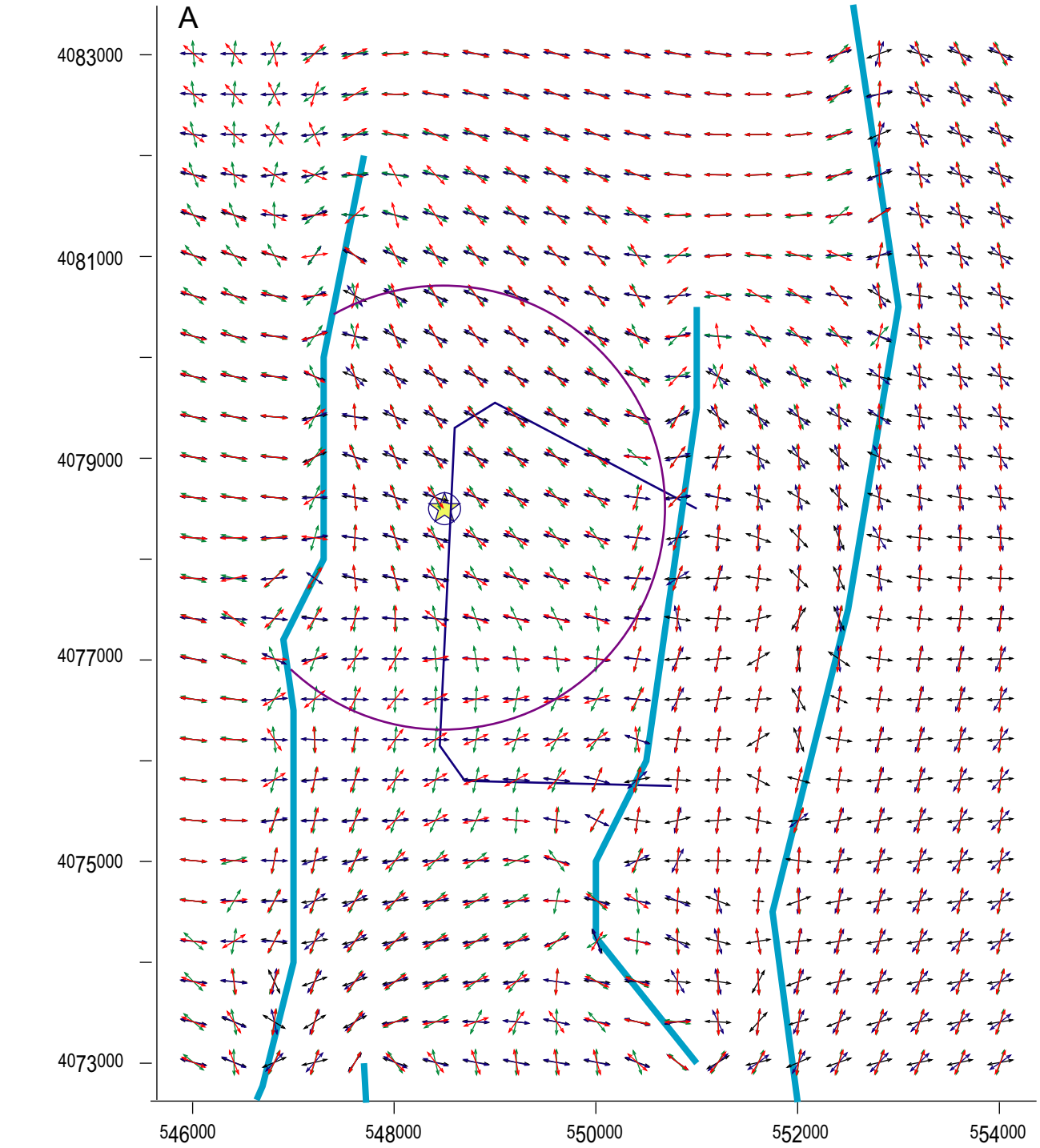

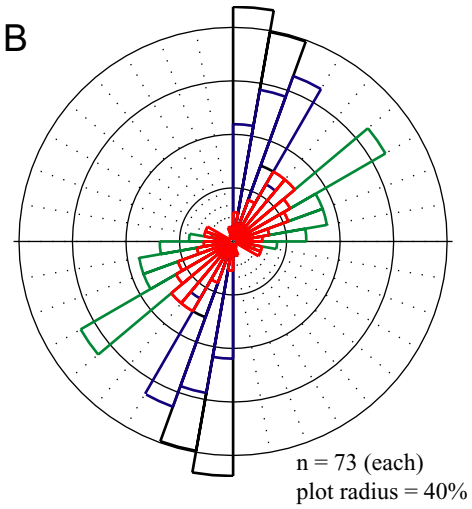

Figure DR5. **A.** Modeled direction of horizontal least principal stress (S_h) at 100 m depth for four different remote stress boundary conditions. In all cases the remote stresses are oriented such that S_h is E-W and S_H is N-S. The shear modulus is 30 GPa. Remote boundary conditions are as in Figs. DR2 and DR3. Black, case A: S_h = L-10, $S_H = S_V$ = L; Blue, case B: S_h = L -10, S_H = L-4; Red, case C: S_h = L -10, S_H = L-8 (These are the results presented in the manuscript.); Green, case D: $S_h = S_H$ = L-10. Faults, features and coordinates as in Fig. DR4. Purple arc encircles data plotted in B. Note that all four trials result in rotation of the stress directions in the vicinity of Live Yucca Ridge (star). **B.** Rose diagram illustrating the expected strikes of first-formed joints within 2 km of Live Yucca Ridge for each of the four modeling scenarios. Colors as above. Case C (red) shows the greatest relative dispersion in joint orientations but also the best match (of the four cases) to reported field observations.

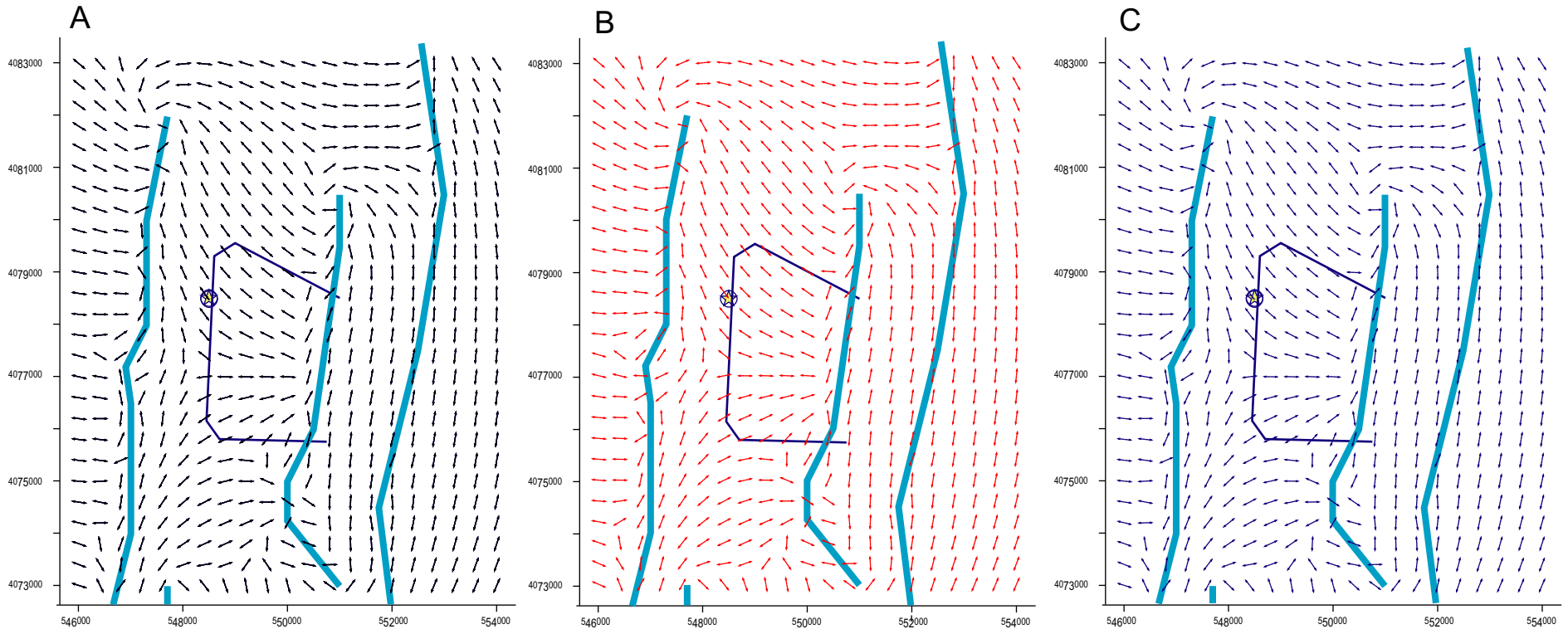

Figure DR6. Identical results of modeled direction of horizontal least principal stress (S_h) at 100 m depth for widely varying elastic moduli. In all cases the remote stresses are oriented such that S_h is E-W and S_H is N-S, and S_h = L -10, S_H = L-8 (case C in Figs. DR2 and DR3.) Faults, features and coordinates as in Fig DR4. **A.** Shear modulus = 3 GPa. **B.** Shear modulus = 30 GPa. (This is the result presented in the manuscript.) **C.** Shear modulus = 100 GPa. The changing shear modulus will influence the total slip on the faults (lower shear modulus, more slip), but the relative amount of slip and slip distribution patterns do not change. Thus, the stress trajectories are not influenced by changing shear modulus.

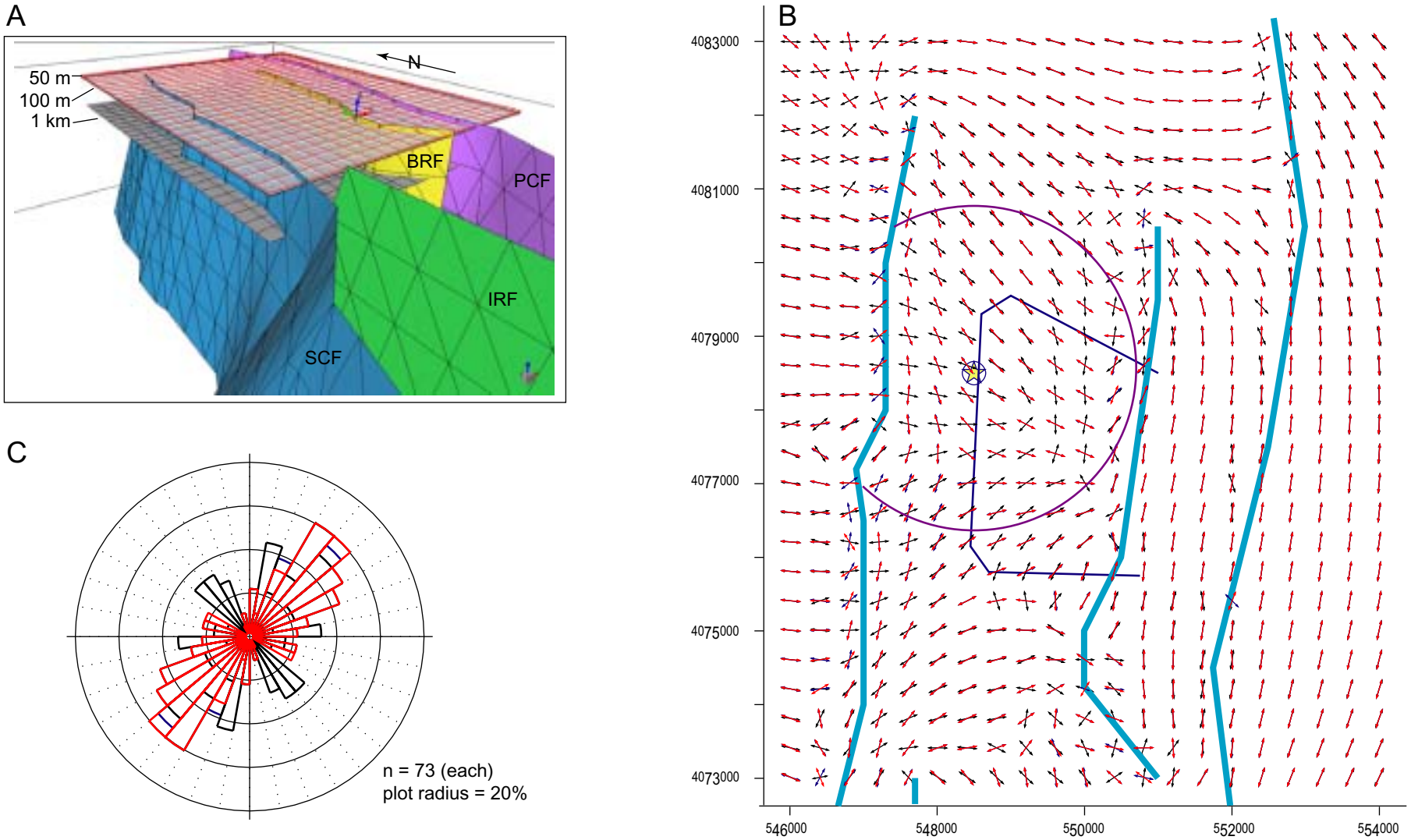

Figure DR7. Modeled direction of horizontal least principal stress (S_h) at various depths. In all cases the remote stresses are oriented such that S_h is E-W and S_H is N-S, and S_h = L -10, S_H = L-8 (case C in Figs. DR2 and DR3.) Shear modulus is 30 GPa. **A.** Perspective model view, looking northeast, showing relative position of three observation planes. Red grid is at 50 m depth. Light grey plane with white grid is at 100m depth. Grey plane with black grid is at 1 km depth. Labels as in Fig. DR1. **B.** Stress trajectories. Blue: 50 m (mostly obscured by red). Red: 100 m. (This is the result presented in the manuscript.) Black: 1 km depth. Faults, features and coordinates as in Fig DR4. Purple arc shows region of data plotted in C. **C.** Rose diagram illustrating the expected strikes of first-formed joints within 2 km of Live Yucca Ridge at each depth. Colors as above. Although the relative magnitudes of the remote horizontal stresses are the same at each depth, the fault geometry varies, and this influences the stress orientations.

Acknowledgements: Stress trajectories and slip distributions were calculated using Poly3D, a three-dimensional boundary element numerical model by Thomas (1993). These results were produced by Poly3d.c (beta), available from the Stanford University Rock Fracture Project (http://pangea.stanford.edu/geomech). Figures DR1a, DR2, DR3, and DR7a were produced using Poly3dGUI, also available from the Stanford Rock Fracture Project. Trajectory plots and rose diagrams were produced using MATLAB (The Mathworks, Inc.). Rose diagrams were generated using a routine modified from Middleton (1999).

Cited references:

Day, W.C., Dickerson, R.P., Potter, C.J., Sweetkind, D.S., San Juan, C.A., Drake, II, R.M., and Fridrich, C.J., 1998, Geologic map of the Yucca Mountain Area, Nye County, Nevada: United States Geological Survey, Geological Investigations Series I-2627, Scale 1:24,000, 1 sheet.

Middleton, G.V., 1999, Data analysis in the Earth Sciences using MATLAB. Prentice Hall, 260 pp.

Thomas, A.L., 1993, Poly3D: A three-dimensional, polygonal-element, displacement discontinuity boundary element computer program with applications to fractures, faults and cavities in Earth's crust [M.S. thesis], Stanford, CA, Stanford University.